

DBConformer: Dual-Branch Convolutional Transformer for EEG Decoding

Ziwei Wang, Hongbin Wang, Tianwang Jia, Xingyi He, Siyang Li, and Dongrui Wu*, *Fellow, IEEE*

Abstract—Electroencephalography (EEG)-based brain-computer interfaces (BCIs) transform spontaneous/evoked neural activity into control commands for external communication. While convolutional neural networks (CNNs) remain the mainstream backbone for EEG decoding, their inherently short receptive field makes it difficult to capture long-range temporal dependencies and global inter-channel relationships. Recent CNN-Transformer (Conformers) hybrids partially address this issue, but most adopt a serial design, resulting in suboptimal integration of local and global features, and often overlook explicit channel-wise modeling. To address these limitations, we propose DBConformer, a dual-branch convolutional Transformer network tailored for EEG decoding. It integrates a temporal Conformer to model long-range temporal dependencies and a spatial Conformer to extract inter-channel interactions, capturing both temporal dynamics and spatial patterns in EEG signals. A lightweight channel attention module further refines spatial representations by assigning data-driven importance to EEG channels. Extensive experiments on five motor imagery (MI) datasets and two seizure detection datasets under three evaluation settings demonstrate that DBConformer consistently outperforms 10 competitive baseline models, with over $8\times$ fewer parameters than the high-capacity EEG Conformer baseline. Further, the visualization results confirm that the features extracted by DBConformer are physiologically interpretable and aligned with sensorimotor priors in MI. The superior performance and interpretability of DBConformer make it reliable for robust and explainable EEG decoding. Code is publicized at <https://github.com/wzwvv/DBConformer>.

Index Terms—Brain-computer interface, electroencephalography, motor imagery, seizure detection, convolutional neural networks, Transformer

I. INTRODUCTION

A brain-computer interface (BCI) provides a direct communication pathway between cortical activity and external devices [1]. Non-invasive BCIs based on electroencephalography (EEG) have gained prominence because EEG sensors are inexpensive, portable, and safe for extended use [2]. Nevertheless, the low signal-to-noise ratio, non-stationarity, and significant inter-subject variability of scalp EEG impose stringent requirements on the decoding model that translates raw signals into task-relevant information. This study focuses on two significant EEG decoding tasks: motor imagery (MI)

classification [3], which enables hands-free control of prostheses and wheelchairs, and epileptic seizure detection [4], a task of automated neurological monitoring.

During MI, users imagine the movement of specific body parts (e.g., left hand, right hand, both feet, or tongue), producing event-related desynchronization/synchronization patterns over the brain’s motor cortex [5]. Despite substantial progress, decoding MI from EEG signals remains challenging.

Epilepsy, affecting over 70 million people worldwide [6], is characterized by recurrent seizures. Continuous EEG monitoring remains the gold standard for seizure detection, but manual annotation by doctors is labor-intensive and costly. Automatic seizure detection must cope with heterogeneous seizure morphologies, varying recordings, and scarce labeled data [7].

Decoding models are essential for effective EEG decoding and has been a research hotspot of BCIs. Three trends have emerged in the design of EEG decoding models:

- 1) *Model Type*: Classic models based on convolutional neural networks (CNNs), such as EEGNet [8], SCNN, and DCNN [9], exploit local spatio-temporal patterns but struggle with global temporal dependencies. CNN-Transformer hybrids (Conformers) extend CNN locality with self-attention based global context. Yet, prior work [10]–[13] largely stacks the two modules serially, restricting interaction between local and global representations and neglecting explicit spatial modeling.
- 2) *Architecture Parallelism and Depth*: Networks evolve from shallow, single-branch (e.g., EEGNet) to deeper, multi-branch designs with more parameters and layers that process frequency bands or multi-resolution inputs in parallel (e.g., FBCNet [14], IFNet [15], and ADFCNN [16]), enhancing feature diversity.
- 3) *Multi-View Information Fusion*: Recent studies consider incorporating temporal, spatial, or spectral domain priors explicitly, such as EEG data augmentation [17], [18], time-frequency transforms [19], [20], frequency band modeling [15], [21], and spatial filtering initialization [22]. However, existing approaches typically consider these domain priors separately rather than jointly.

Overall, the latest serial Conformer hybrids first compress EEG trials into patch embeddings by CNN blocks and then utilize self-attention to capture global long-range dependencies. While effective for certain tasks, this cascade forces all spatial information to pass through a temporal bottleneck, preventing interaction between local and global characteristics. Notably, some Conformer hybrids have large model sizes, e.g., EEG Conformer contains around 0.8M parameters, which increases

This research was supported by Shenzhen Science and Technology Innovation Program JCYJ20220818103602004, and Zhongguancun Academy 20240301.

Z. Wang, H. Wang, T. Jia, X. He, S. Li, and D. Wu are with the Ministry of Education Key Laboratory of Image Processing and Intelligent Control, School of Artificial Intelligence and Automation, Huazhong University of Science and Technology, Wuhan 430074, China. Z. Wang H. Wang, T. Jia, S. Li, and D. Wu are also with the Shenzhen Huazhong University of Science and Technology Research Institute, Shenzhen, 518000 China.

*Corresponding Author: Dongrui Wu (drwu@hust.edu.cn).

computational cost and may overfit on limited EEG data. Besides, spatial inter-channel relationships, often captured in early CNN layers, may be overwhelmed in later blocks, limiting the model’s capacity to leverage spatial information crucial for MI classification and seizure detection. A balanced, parallel design that treats temporal and spatial patterns symmetrically remains absent.

To address the above limitations, we propose DBConformer, a dual-branch convolutional Transformer architecture that performs parallel spatio-temporal representation learning for EEG decoding. The temporal Conformer (T-Conformer) extracts hierarchical temporal dynamics by coupling depthwise temporal convolutions with multi-head self-attention, whereas the spatial Conformer (S-Conformer) leverages pointwise convolutions and channel-wise self-attention to model spatial dependencies. A lightweight channel attention module adaptively refines spatial saliency before branch fusion. In each branch, CNN extracts temporal/spatial local representations, and Transformer captures global dependencies in the temporal or channel horizon. The comparison of network architectures among CNNs, traditional serial Conformers, and the proposed DBConformer, illustrated in Fig. 1.

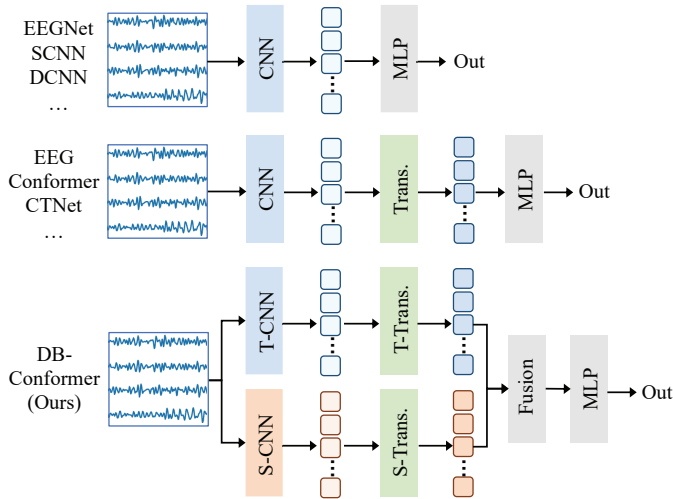


Fig. 1. Comparison of network architectures among CNNs (EEGNet [8], SCNN [9], DCNN [9], etc), traditional serial Conformers (EEG Conformer [10], CTNet [11], etc), and the proposed DBConformer. DBConformer has two branches that parallel capture temporal and spatial characteristics.

The main contributions of this work are summarized as follows:

- 1) We propose DBConformer, a dual-branch convolutional Transformer network for EEG decoding. It incorporates a temporal branch T-Conformer and a spatial branch S-Conformer, enabling simultaneous modeling of temporal dynamics and spatial patterns in EEG signals.
- 2) A lightweight, plug-and-play channel attention module is introduced to learn the relative importance of each EEG channel in a data-driven manner. This module reweights spatial features before fusion, enhancing both classification accuracy and interpretability without requiring additional supervision.

- 3) Extensive experiments on five MI datasets and two seizure detection datasets validated that DBConformer consistently outperforms 10 competitive baseline models. Furthermore, it achieves this superior performance with over $8\times$ fewer parameters than the high-capacity EEG Conformer baseline, demonstrating both effectiveness and efficiency.
- 4) Beyond achieving state-of-the-art performance, DBConformer exhibits biological interpretability, i.e., its learned channel attention scores consistently emphasize sensorimotor-related electrodes (e.g., C3, Cz, C4), aligning well with known neurophysiological priors.

The remainder of this paper is organized as follows: Section II reviews related works. Section III details the proposed DBConformer. Section IV discusses the experimental results and provides analyses. Section V draws conclusions.

II. RELATED WORKS

EEG decoding has progressed from traditional hand-crafted pipelines to large-scale, end-to-end deep learning architectures. Recent advancements focus on the model design, including CNN-based, CNN-Transformer hybrid, and the emerging CNN-Mamba architectures. A review of current EEG decoding models is shown in Table I.

Early approaches to MI classification heavily relied on spatial filtering [23] to maximize inter-class variance. In automatic seizure detection, prior features were manually extracted and classified by classifiers such as support vector machines [24] and random forest [25]. These pipelines required substantial domain expertise and manual effort for feature extraction, motivating a shift toward end-to-end deep learning models.

A. CNNs

CNNs are well-suited for modeling the local spatio-temporal characteristics of EEG data. Lightweight CNN models such as EEGNet [8], SCNN [9], FBCNet [14], and IFNet [15] achieve competitive performance with relatively few parameters. FBM-SNet [21] employs multi-scale convolutional blocks to enlarge the receptive field by parallelizing convolutions across different frequency bands. EEGWaveNet [26] introduces a multi-scale temporal CNN architecture with depthwise filters that are channel-specific, extracting multi-scale features from trials of each EEG channel for seizure detection. However, the inherently local nature of convolutional kernels limits their ability to capture long-range temporal dependencies and global spatial patterns.

B. Serial CNN-Transformer Hybrids

To incorporate global information, recent models augment CNNs with Transformers, typically in a serial architecture. For example, EEG Conformer [10], CTNet [11], EEG-Deformer [12], and SE-TSS-Transformer [13] compress EEG trials into patch embeddings using convolutional blocks and subsequently apply Transformer layers to capture long-range dependencies. However, this serial design constrains information flow to a single pathway, where local and global features

TABLE I
A REVIEW OF CURRENT EEG DECODING MODELS.

Model Type	Model Name	Model Structure	# Branches	Explicit Information Fusion	Paradigms
CNN	EEGNet [8]	Serial	1	No	MI
	SCNN [9]	Serial	1	No	MI
	DCNN [9]	Serial	1	No	MI
	FBCNet [14]	Parallel	1	Spectral	MI
	FBMSNet [21]	Parallel	4	Spectral	MI
	IFNet [15]	Parallel	2	Spectral	MI
	ADFCNN [16]	Parallel	2	No	MI
EEGWaveNet [26]	Parallel	5	No	Seizure detection	
CNN-Mamba	EEGMamba [27]	Serial	1	No	MI, seizure detection, sleep stage classification, and emotion recognition
	MI-Mamba [28]	Serial	1	No	MI
	EEG VMamba [29]	Serial	1	No	Seizure prediction
	SlimSeiz [30]	Serial	1	No	Seizure prediction
	BiT-MamSleep [31]	Serial	1	No	Sleep stage classification
CNN-Transformer	EEG Conformer [10]	Serial	1	No	MI, emotion recognition
	CTNet [11]	Serial	1	No	MI
	EEG-Deformer [12]	Serial	1	No	Event-related potentials
	SE-TSS-Transformer [13]	Serial	1	No	Seizure detection
	MVCNet [17]	Parallel	2	Temporal, spatial, and spectral	MI
	DBConformer (Ours)	Parallel	2	Temporal, spatial	MI, seizure detection

are processed sequentially. As a result, spatial inter-channel relationships, often captured in early CNN layers, may be overwhelmed in later blocks, limiting the model’s capacity to leverage spatial information.

C. Other Architectures

Mamba [32], a recently proposed alternative to Transformers, provides efficient modeling of long-range dependencies with reduced computational cost. EEGMamba [27] and MI-Mamba [28] integrate Mamba blocks following CNN layers, adhering to the same serial structure of CNN-Transformer hybrids. However, parallel architectures that jointly model temporal and spatial patterns remain underexplored.

Some research explores architectures beyond CNNs, including full self-attention mechanisms [33] and graph neural networks [34]–[36]. Transformer-based models capture long-range dependencies, and graph neural networks leverage electrode topology to refine spatial characteristics. These models are typically parameter-intensive and rarely integrate local feature extraction with global modeling.

Overall, CNNs excel at modeling local spatio-temporal features. CNN-Transformer and CNN-Mamba hybrids offer broader temporal modeling but are limited by the serial design, overlooking the interaction between local and global representations, as well as the spatial patterns.

III. DBCONFORMER

A. Overview

This section details the proposed DBConformer, illustrated in Fig. 2. In contrast to conventional single-branch EEG decoding networks, such as CNN-based models or serial CNN-Transformer hybrids, DBConformer adopts a parallel dual-branch structure to better leverage the advantages of CNN

and Transformer. Specifically, T-Conformer captures long-range temporal dependencies, and S-Conformer models inter-channel relations. A lightweight channel attention module is further incorporated to enhance spatial representations by assigning adaptive, data-driven weights to individual EEG channels. The outputs from both branches are concatenated and fed into the classifier to obtain the final predictions.

B. Data Normalization

The raw EEG trials of a batch are $\mathbf{X} \in \mathbb{R}^{B \times C \times T}$, where B is the batch size, C the number of channels, and T the number of time samples. We apply Euclidean alignment (EA) [37] to align the original trials from each subject in the Euclidean space. Assume a subject has n trials, EA can be formulated as:

$$\tilde{X}_i = \bar{R}^{-1/2} X_i, \quad (1)$$

where \bar{R} is the arithmetic mean of all covariance matrices from a subject:

$$\bar{R} = \frac{1}{n} \sum_{i=1}^n X_i X_i^T. \quad (2)$$

After EA, data distribution discrepancies from different subjects are effectively decreased.

C. Network Architecture

The detailed architecture of DBConformer is summarized in Table II, outlining the composition of each module. As shown in Fig. 2 and Table II, DBConformer is composed of T-Conformer and S-Conformer branches, along with a classification module. A channel attention module is integrated in S-Conformer for channel-aware weighting.

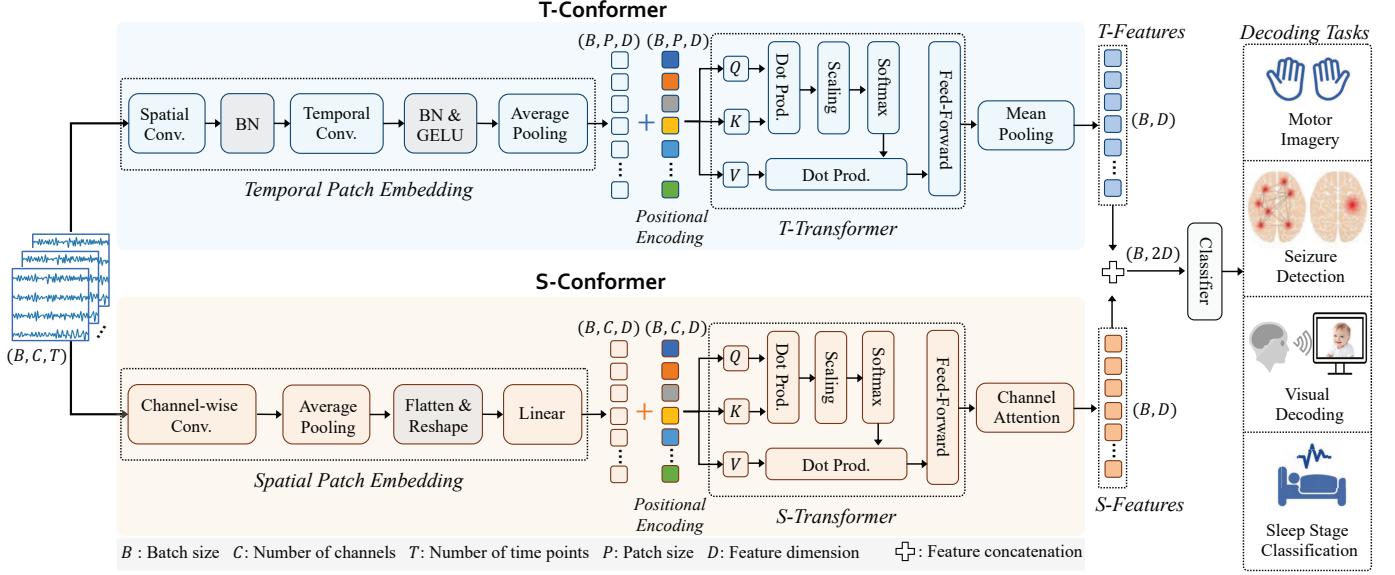


Fig. 2. The architecture of proposed DBConformer for EEG decoding.

TABLE II
DBCONFORMER ARCHITECTURE.

Branch	Module	Layer	# Kernels	Kernel Size	# Parameters	Output Shape	Options	
T-Conformer	Temporal Patch Embedding	Separable Conv1D	F	$(1,)$	$C \cdot F$	(B, F, T)	Spatial filtering	
		BatchNorm1D	–	–	$2F$	(B, F, T)	Normalization	
		Temporal Conv1D	F	$(K,)$	$F \cdot K$	(B, F, T)	Temporal depthwise Conv.	
		BatchNorm1D & GELU	–	–	$2F$	(B, F, T)	Normalization and non-linearity	
		Dropout	–	–	0	(B, F, T)	$p = 0.5$	
		AvgPool1D	–	$(1, W)$	0	(B, F, P)	Patch-wise downsampling	
		Permute	–	–	0	(B, P, F)	Patch tokens along time axis	
T-Conformer	T-Transformer	Positional Encoding	–	–	$P \cdot D$	(B, P, D)	Learnable temporal encoding	
		Transformer Encoder	–	–	\sim	(B, P, D)	L_t layers, H_t heads	
		Mean Pooling	–	–	0	(B, D)	Mean over patches	
S-Conformer	Spatial Patch Embedding	Channel-wise Conv1D	16	25	–	$(B \cdot C, 16, T')$	Per-channel temporal filtering	
		AvgPool1D	–	–	0	$(B \cdot C, 16, 1)$	Channel-wise downsampling	
		Flatten	–	–	0	$(B \cdot C, 16)$	Reshape	
		Reshape	–	–	0	$(B, C, 16)$	Channel-token preparation	
		Linear	16	–	$16D$	(B, C, D)	Project to embedding space	
	S-Conformer	S-Transformer	Positional Encoding	–	–	$C \cdot D$	(B, C, D)	Learnable spatial encoding
			Transformer Encoder	–	–	\sim	(B, C, D)	L_s layers, H_s heads
		Channel Attention	Linear	–	–	$D \cdot D$	(B, C, D)	Intermediate token projection
			Tanh	–	–	0	(B, C, D)	Non-linearity
			Linear	–	–	D	$(B, C, 1)$	Channel-level scoring
Softmax	–		–	0	$(B, C, 1)$	Normalize across channels		
	Weighted Summation	–	–	0	(B, D)	Weighted channel-aware feature		
/	Fusion	Concatenation	–	–	0	$(B, 2D)$	Feature fusion	
		Classifier	FC Layers	–	–	$2D \rightarrow 64 \rightarrow 32 \rightarrow N_c$	(B, N_c)	3-layer MLP (ELU, Dropout)

B : batch size, C : number of channels, T : number of time points, T' : temporal length after Conv1D, F : number of filters, K : temporal kernel size, W : pooling window size, $P = T/W$: number of temporal patches, D : embedding dimension, L_t : number of T-Transformer encoder layers, L_s : number of S-Transformer encoder layers, H_t : number of T-Transformer encoder heads, H_s : number of S-Transformer encoder heads, N_c : number of classes.

1) *T-Conformer*: The temporal branch of DBConformer, termed T-Conformer, is designed to capture fine-grained temporal dependencies in EEG trials. It comprises two primary components: a convolutional patch embedding module and a T-Transformer encoder.

a) *Temporal Patch Embedding*: Inspired by prior CNN backbones in EEG decoding [15], we design the module with a depthwise separable 1D convolution, a 1D temporal convolution, and an average pooling layer. The first separable convolution has F kernels with a stride of $(1, \cdot)$, followed with batch normalization. The second temporal convolution applies F filters, accompanied by batch normalization, a GELU activation, and a dropout with a probability $p = 0.5$. Then, an average pooling with kernel size $(1, W)$ is applied along the time dimension to form non-overlapping temporal patches \mathbf{Z}_t . Finally, the patches are reshaped via transposition. The number of filters F is set equal to the Transformer embedding dimension D , thereby eliminating the need for a separate linear projection.

b) *Temporal Transformer Encoder*: The extracted patches \mathbf{Z}_t pass through a Transformer encoder [38] to model temporal dependencies. We add a learnable positional encoding $\mathbf{E}_t^{\text{pos}} \in \mathbb{R}^{1 \times P \times D}$ to preserve temporal ordering:

$$\mathbf{Z}_t^{\text{in}} = \mathbf{Z}_t + \mathbf{E}_t^{\text{pos}}. \quad (3)$$

A lightweight Transformer encoder with L_t layers and H_t attention heads is then applied:

$$\mathbf{Z}_t^{\text{out}} = \text{TransformerEncoder}(\mathbf{Z}_t^{\text{in}}) \in \mathbb{R}^{B \times P \times D}. \quad (4)$$

To aggregate temporal patch features into a global representation, we employ mean pooling over the patch dimension:

$$\mathbf{F}_t = \frac{1}{P} \sum_{i=1}^P \mathbf{Z}_t^{\text{out}}[:, i, :] \in \mathbb{R}^{B \times D}, \quad (5)$$

which is the final temporal representations of input EEG trials.

2) *S-Conformer*: The spatial branch of DBConformer, termed S-Conformer, is designed to extract inter-channel spatial patterns. It consists of three components: a convolutional spatial patch embedding, an S-Transformer encoder, and a channel attention module.

a) *Spatial Patch Embedding*: This module transforms each EEG trial into a spatial token embedding. A depthwise 1D convolution across the time dimension is designed to extract short-range temporal features per channel. Next, average pooling is applied over the temporal dimension to summarize each channel's temporal response, yielding a compressed representation. Then, patches are flattened and reshaped to restore batch and channel dimensions. Finally, a linear projection layer is applied to map each channel token to the desired embedding dimension D .

b) *Spatial Transformer Encoder*: To capture global spatial dependencies across EEG channels, the embedded channel tokens \mathbf{Z}_s are processed by a lightweight Transformer encoder. A learnable positional encoding $\mathbf{E}_s^{\text{pos}} \in \mathbb{R}^{1 \times C \times D}$ is added to retain channel ordering:

$$\mathbf{Z}_s^{\text{in}} = \mathbf{Z}_s + \mathbf{E}_s^{\text{pos}}. \quad (6)$$

Then, a Transformer encoder with L_s layers and H_s heads is applied:

$$\mathbf{Z}_s^{\text{out}} = \text{TransformerEncoder}(\mathbf{Z}_s^{\text{in}}) \in \mathbb{R}^{B \times C \times D}. \quad (7)$$

c) *Channel Attention*: A lightweight channel attention module are proposed to adaptively refining the spatial saliency of features from S-Conformer, illustrated in Fig. 3.

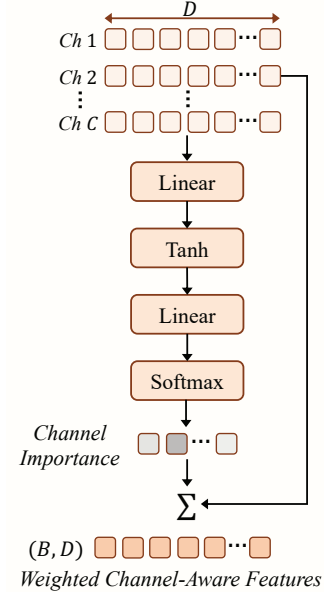


Fig. 3. Details of the proposed channel attention module.

Specifically, each token $\{z_i^c\}_{c=1}^C$ of $\mathbf{Z}_s^{\text{out}}$ is projected through two fully connected layers:

$$k_i^c = \mathbf{w}_2^\top \tanh(\mathbf{W}_1 z_i^c), \quad (8)$$

where $\mathbf{W}_1 \in \mathbb{R}^{D \times D}$ and $\mathbf{w}_2 \in \mathbb{R}^D$ are learnable parameters, and $\tanh(\cdot)$ is the non-linear activation function. The attention weights are then obtained via Softmax normalization:

$$\alpha_i^c = \frac{\exp(k_i^c)}{\sum_{j=1}^C \exp(k_i^j)}, \quad c = 1, \dots, C. \quad (9)$$

Then, each token is transformed into attention-weighted sum across channels:

$$\mathbf{f}_s, i = \sum_{c=1}^C \alpha_i^c \cdot \mathbf{z}_i^c. \quad (10)$$

By repeating across all B samples in a batch, the final batch-level spatial representation $\mathbf{F}_s \in \mathbb{R}^{B \times D}$ can be obtained.

3) *Feature Fusion and Classification*: After obtaining the representations from the temporal and spatial branches, i.e., $\mathbf{F}_t \in \mathbb{R}^{B \times D}$ from T-Conformer and $\mathbf{F}_s \in \mathbb{R}^{B \times D}$ from S-Conformer, the two features are concatenated along the feature dimension to form the fused representation:

$$\mathbf{F}_{\text{fused}} = [\mathbf{F}_t; \mathbf{F}_s] \in \mathbb{R}^{B \times 2D}, \quad (11)$$

which is then passed through a multi-layer perceptron classifier to generate the final predictions \hat{y}_i . The classifier consists of three fully connected layers with intermediate ELU activations and dropout regularization.

Given the prediction \hat{y}_i and the ground-truth label y_i , the classification loss is:

$$\mathcal{L}_{CLS} = \frac{1}{B} \sum_{i=1}^B \text{CE}(\hat{y}_i, y_i), \quad (12)$$

where $\text{CE}(\cdot, \cdot)$ denotes the cross-entropy loss function and B is the batch size.

IV. EXPERIMENTS AND RESULTS

This section details the datasets, experiments, and analyses. We implemented and fairly evaluated ten state-of-the-art EEG decoding models, including CNN-based, CNN-Transformer hybrid, and CNN-Mamba hybrid. Code for DBConformer, along with all compared baseline models, is available on GitHub¹, serving as a benchmark codebase for EEG decoding.

A. Datasets

We conducted experiments on two EEG decoding tasks: MI classification and epileptic seizure detection. Characteristics of all datasets are summarized in Table III.

1) *MI Datasets*: We adopted five publicly available MI datasets from the MOABB benchmark [39] and BCI competitions:

- BNCI2014001 [40]: Contains EEG trials from 9 subjects performing left/right hand MI, recorded with 22 EEG channels at 250 Hz. The first session was used in the experiments.
- BNCI2014004 [41]: Contains EEG trials from 9 subjects performing left/right hand MI, recorded with only 3 EEG channels at 250 Hz. The first session was used in the experiments.
- Zhou2016 [42]: Comprises EEG trials from 4 subjects performing left/right hand MI, recorded with 14 channels at 250 Hz. The first session was used in the experiments.
- Blankertz2007 [43]: From BCI Competition IV dataset 1, includes 7 subjects with 59-channel EEG sampled at 250 Hz. Subjects 1 and 5 performed left hand/right foot MI, and the other five subjects performed left/right hand MI.
- BNCI2014002 [44]: Includes 14 subjects, each performing eight runs right hand/feet MI, using 15 EEG channels recorded at 512 Hz. The first five training runs were used in the experiments.

2) *Seizure Detection Datasets*: Two clinical seizure detection datasets are evaluated:

- CHSZ [7]: Contains EEG recordings from 27 pediatric patients aged 3 months to 10 years, recorded with 19 unipolar electrodes at a sampling rate of 500 or 1000 Hz. All recordings were manually annotated by neurologists to mark the onset and termination of seizures.
- NICU [45]: A large-scale neonatal EEG dataset collected from 79 full-term neonates in the Helsinki University Hospital neonatal intensive care unit. Data were recorded at 256 Hz, with the same electrodes as CHSZ. Seizures were independently annotated by three clinical experts

with a 1s window. A consensus set comprising 39 neonates with confirmed seizures was utilized in the experiments.

3) *Data Preprocessing*: For BNCI2014001, BNCI2014004, Zhou2016, and BNCI2014002 datasets, the standard preprocessing steps in MOABB, including notch filtering, band-pass filtering, etc., were performed to ensure the reproducibility. For the Blankertz2007 dataset, EEG trials were first band-pass filtered between 8 and 30 Hz. Then, trials between [0.5, 3.5] seconds after the cue onset were segmented and downsampled to 250 Hz.

For seizure datasets, 18 bipolar channels were first generated from 19 unipolar channels, following [45]. And EEGs were segmented into 4s non-overlapping trials. Then, trials from both datasets were preprocessed by a 50 Hz notch filter and a 0.5-50 Hz bandpass filter. For CHSZ, 1000 Hz trials were downsampled to 500 Hz for consistency. For NICU, the ground truth label of each trial was determined by the majority vote of three experts.

EA was utilized after pre-processing on all datasets, and the EA reference matrix was updated online when new test trials arrived on-the-fly, as in [46].

B. Compared Approaches

Ten EEG decoding models were reproduced and compared with the proposed DBConformer.

- EEGNet [8] is a compact CNN tailored for EEG classification. It includes two key convolutional blocks: a temporal convolution for capturing frequency-specific features, followed by a depthwise spatial convolution. A separable convolution and subsequent pointwise convolution are designed to enhance spatio-temporal representations.
- SCNN [9] is a shallow CNN inspired by the filter bank common spatial pattern, utilizing temporal and spatial convolutions in two stages to efficiently extract discriminative EEG features.
- DCNN [9] is a deeper version of SCNN with larger parameters, consisting of four convolutional blocks with max pooling layers.
- FBCNet [14] incorporates spatial convolution and a temporal variance layer to extract spectral-spatial features across multiple EEG frequency bands.
- ADFCNN [16] is a dual-branch CNN model employing multi-scale temporal convolutions for frequency domain analysis and separable spatial convolutions for global spatial feature extraction. Features from both branches are fused using attention-based fusion before being fed into a fully connected classification head.
- CTNet [11] combines a convolutional front-end, similar to EEGNet, with a Transformer encoder for capturing long-range dependencies in EEG data. This serial structure enhances both local and global feature learning.
- EEG Conformer [10] integrates a convolutional block, a Transformer encoder block, and a classifier. The convolutional block is equipped with temporal and spatial convolutional layers, followed by an average pooling

¹<https://github.com/wzwvvv/DBConformer>

TABLE III
SUMMARY OF THE FIVE MI DATASETS AND TWO SEIZURE DATASETS.

Paradigm	Dataset	Number of Subjects	Number of EEG Channels	Sampling Rate (Hz)	Trial Length (seconds)	Number of Total Trials	Task Types
MI	BNCI2014001	9	22	250	4	1,296	left/right hand
	BNCI2014004	9	3	250	5	1,080	left/right hand
	Zhou2016	4	14	250	5	409	left/right hand
	Blankertz2007	7	59	250	3	1,400	left/right hand or left hand/right foot
	BNCI2014002	14	15	512	5	1,400	right hand/both feet
Seizure detection	CHSZ	27	19	500 or 1,000	4	21,237	normal/seizure
	NICU	39	19	256	4	52,534	normal/seizure

layer. CNN, Transformer, and the classifier are serially equipped, similar to CTNet.

- SlimSeiz [30] integrates multiple 1D CNN layers to extract features at various temporal resolutions and a Mamba block to capture long-range temporal dependencies for seizure prediction. SlimSeiz enhances temporal modeling by integrating the Mamba block while avoiding a significant parameter overhead.
- IFNet [15] extends the spectral-spatial approach by decomposing EEG into multiple frequency bands (e.g., 4-16 Hz, 16-40 Hz). For each band, it applies 1D spatial and temporal convolutions, followed by feature concatenation and a fully connected layer for classification.
- EEGWaveNet [26] introduces a multi-scale temporal CNN architecture with depthwise filters that are channel-specific, extracting multi-scale features from trials of each EEG channel.

C. Implementation

1) *Evaluation Scenarios*: To evaluate the performance under different conditions, we performed three experimental settings: chronological order (CO), cross-validation (CV), and leave-one-subject-out (LOSO), covering both within-subject and cross-subject settings, as in [17].

- CO: Trials from each subject were split according to recording time. The first 80% trials were used for training, and the remaining 20% for testing. This scenario reflects a within-subject evaluation protocol that mimics real-time deployment.
- CV: A 5-fold cross-validation was adopted, where the dataset was divided chronologically into five equal parts with balanced classes. In each iteration, four folds were used for training and one for testing. This also constitutes a within-subject setting, following the protocol in [14].
- LOSO: EEG trials from a single subject were held out as the test set, while data from all remaining subjects were joint for training. This setting evaluates the model’s cross-subject decoding ability.

2) *Evaluation Metrics*: Accuracy is employed to evaluate the performance on five MI datasets. Accuracy is the overall proportion of correctly classified trials, regardless of class:

$$Accuracy = \frac{TP + TN}{TP + TN + FP + FN} \times 100\%, \quad (13)$$

where TP is the number of correctly classified positive trials, TN the number of correctly classified negative trials, FP the

number of negative trials misclassified as positive, and FN the number of positive trials misclassified as negative.

To evaluate the classification performance on class-imbalanced seizure datasets, three additional metrics are included.

- Area under the receiver operating characteristic curve (AUC) is a threshold-independent metric that reflects the model’s ability to distinguish between seizure and non-seizure trials across varying decision thresholds.
- F1 Score is the harmonic mean of precision and recall, indicating the balance between false positives and false negatives:

$$F1 = \frac{2TP}{2TP + FP + FN} \times 100\%. \quad (14)$$

- Balanced classification accuracy (BCA) is the average of sensitivity and specificity, which accounts for class imbalance:

$$BCA = \frac{sensitivity + specificity}{2} \times 100\%, \quad (15)$$

where $sensitivity = \frac{TP}{TP + FN}$ is the proportion of correctly detected seizure trials, and $specificity = \frac{TN}{TN + FP}$ is the proportion of correctly detected normal trials.

3) *Parameter Settings*: All experiments were repeated five times with a random seed list [1, 2, 3, 4, 5], and the average results were reported. For all MI datasets, models were trained for 100 epochs using the Adam optimizer with a learning rate 10^{-3} and a batch size of 32. For seizure datasets, models are trained for 200 epochs using the Adam optimizer with a learning rate 10^{-3} . The batch size was set to 256 for CHSZ and 512 for NICU because of the larger data size. Due to the specific characteristics of datasets, scenarios, and tasks, we adopted distinct model configurations accordingly, as summarized in Table IV.

D. Results on MI Classification

Table V presents the average classification accuracies of DBConformer and nine baseline models across five MI datasets under three evaluation settings. Observed that:

- Among the nine baseline models, IFNet achieves the highest average accuracy across all three settings, attributed to its frequency-aware architectural design. EEG Conformer ranks second under the CO and CV settings but exhibits reduced performance in the LOSO scenario,

TABLE IV
MODEL CONFIGURATIONS OF DBCONFORMER FOR EACH DATASET.

Dataset	Patch Size	Embed. Size	# T-Trans. Layers	# T-Trans. Heads	# S-Trans. Layers	# S-Trans. Heads
CO/CV						
BNCI2014001	125	40	2	2	2	2
BNCI2014004	125	40	2	2	2	2
Zhou2016	125	40	2	2	2	2
Blankertz2007	125	40	2	2	2	2
BNCI2014002	128	40	4	2	4	2
LOSO						
BNCI2014001	125	40	2	2	2	2
BNCI2014004	125	40	2	2	2	2
Zhou2016	125	40	6	2	6	2
Blankertz2007	125	40	6	2	6	2
BNCI2014002	128	40	6	2	6	2
CHSZ	100	60	2	2	2	2
NICU	128	60	2	2	2	2

indicating that its large parameter size may cause overfitting when generalizing to unseen subjects.

- Compared to the CO setting, results under CV are generally higher across all models, consistent with findings in [17], where temporally ordered training limits generalization due to potential signal drift or session variance. CV benefits from more diverse training trials within each subject. This highlights the importance of fair and appropriate partitioning when benchmarking EEG decoding models.
- In the LOSO setting, DBConformer maintains the best generalization across subjects. This highlights the robustness of DBConformer in cross-subject EEG decoding tasks.
- DBConformer consistently outperforms all baseline models across all datasets and settings. Compared to classical CNN models, such as EEGNet and FBCNet, DBConformer exhibits significant accuracy gains. Compared with recent CNN-Transformer hybrids (e.g., EEG Conformer and CTNet), DBConformer achieves consistently better results with fewer performance fluctuations. This demonstrates the effectiveness of the dual-branch design in capturing both temporal and spatial characteristics.

E. Results on Seizure Detection

For seizure, we compared the proposed DBConformer with seven baseline models: EEGNet, SCNN, DCNN, ADFCNN, EEG Conformer, SlimSeiz, and EEGWaveNet. The first five models were originally designed for tasks such as MI and emotion recognition, rather than seizure detection. But they are general for all EEG decoding tasks; thus, we re-implemented and adapted them to seizure detection. SlimSeiz [30] is a CNN-Mamba hybrid model for seizure prediction that can be easily implemented in the seizure detection task. EEGWaveNet [26] is a multi-scale depthwise CNN specifically developed for seizure detection, serving as a competitive task-specific benchmark. Table VI summarizes the average AUCs, F1 scores, and BCAs of DBConformer and six baseline models on the CHSZ and NICU datasets. Observed that:

- Among the baseline approaches, EEG Conformer and ADFCNN achieved competitive performance across most metrics. EEG Conformer benefits from its temporal modeling capacity, while ADFCNN leverages dual-scale convolutions to capture frequency-sensitive patterns.
- Compared to CHSZ, all models generally exhibited lower performance on the NICU dataset. This degradation can be attributed to differences in recording conditions, subject age, and seizure morphology. The smaller brain volume of neonates introduces greater variability and reduces the signal-to-noise ratio in NICU, underscoring the need for robust generalization across patients.
- DBConformer achieved the best performance across all evaluation metrics and both datasets. Compared to strong baselines such as EEG Conformer and ADFCNN, DBConformer yielded a 2-4% improvement in BCAs. Results demonstrate the adaptability of DBConformer to clinical EEG decoding tasks. The dual-branch spatio-temporal modeling design provides robust representations for varying patients, making it more reliable for real-world seizure detection.

F. Ablation Study

To further validate the effectiveness of DBConformer’s key components, we conducted ablation studies on the parallel spatio-temporal design, positional encoding, and the channel attention module. Experiments were performed on five MI datasets under three settings, shown in Fig. 4. Observed that:

- *Parallel Spatio-Temporal Modeling.* We compared the full DBConformer (T-Conformer + S-Conformer) with its T-Conformer only variant. Adding the S-Conformer branch consistently improves performance across all settings. Results confirm the effectiveness of incorporating spatial features via the auxiliary S-Conformer, which complements the dominant temporal modeling of T-Conformer.
- *Positional Encoding.* Disabling the learnable positional embeddings for both temporal and spatial tokens results in performance drops under all settings. This validates the importance of explicit temporal/channel ordering when modeling patch and channel tokens.
- *Channel Attention Module.* Replacing the channel attention module with naïve mean pooling degrades performance, confirming that adaptively reweighting EEG channels benefits enhancing spatial features.

G. Effect of Dual-Branch Modeling

To further evaluate the impact of dual-branch architecture, we conducted feature visualization experiments using t -SNE [47]. Features extracted by T-Conformer (temporal branch only) and DBConformer (dual-branch) were compared on four MI datasets, shown in Fig. 5. Observed that:

- *T-Conformer alone exhibits limited separability.* Although T-Conformer captures meaningful temporal structures, its extracted features tend to form overlapping clusters across classes in datasets such as BNCI2014004 and Blankertz2007, which limits class discriminability.

TABLE V

AVERAGE CLASSIFICATION ACCURACIES (%) OF DBCONFORMER AND NINE BASELINE MODELS ON FIVE MI DATASETS UNDER CO, CV, AND LOSO SCENARIOS. THE BEST AVERAGE PERFORMANCE OF EACH DATASET IS MARKED IN BOLD, AND THE SECOND BEST BY AN UNDERLINE.

Scenario	Dataset	EEGNet	SCNN	DCNN	FBCNet	ADFCNN	CTNet	EEG Conformer	SlimSeiz	IFNet	DBConformer
CO	BNCI2014001	69.05±1.00	73.57±2.36	59.29±1.64	68.97±1.26	73.73±2.26	73.49±2.05	<u>78.57</u> ±0.66	68.89±2.05	77.94±0.93	79.05 ±1.82
	BNCI2014004	68.43±2.20	68.15±1.39	62.41±1.64	65.46±1.57	69.63±1.19	71.57±1.33	72.04±1.57	68.24±2.74	<u>73.43</u> ±1.72	75.09 ±1.53
	Zhou2016	80.13±3.35	75.03±6.15	78.03±2.37	63.33±2.29	71.42±1.95	76.81±5.05	73.87±4.51	72.01±3.98	<u>81.70</u> ±2.08	82.49 ±2.40
	Blankertz2007	78.79±2.78	76.71±2.09	70.00±4.12	75.93±1.31	76.07±1.41	79.00±3.38	82.29±2.62	65.64±1.18	<u>84.00</u> ±0.57	87.21 ±1.32
	BNCI2014002	66.07±2.76	<u>79.07</u> ±1.96	64.07±2.70	69.50±0.95	73.00±1.95	71.00±1.80	76.21±1.46	78.71±0.53	78.29±1.68	79.14 ±0.17
	Average	72.49	74.51	66.76	68.64	72.77	74.38	76.59	70.70	<u>79.07</u>	80.60
CV	BNCI2014001	71.86±0.96	78.22±0.19	61.59±1.08	74.74±0.67	77.27±0.60	75.97±0.76	<u>83.62</u> ±0.99	75.56±1.48	82.62±0.91	83.66 ±0.40
	BNCI2014004	68.91±0.86	68.13±0.63	63.51±0.40	67.17±0.30	69.48±1.24	70.96±1.06	<u>73.15</u> ±0.72	69.74±0.46	72.02±0.52	74.17 ±0.63
	Zhou2016	85.30±2.12	82.90±0.90	79.68±1.13	80.01±0.50	84.95±1.51	86.38±1.45	85.67±1.52	85.60±1.36	<u>87.78</u> ±1.01	91.54 ±0.20
	Blankertz2007	80.21±0.77	81.11±0.72	69.83±1.51	84.14±0.67	81.10±1.41	83.64±1.04	87.43±0.33	75.37±1.14	<u>88.23</u> ±0.50	90.33 ±0.53
	BNCI2014002	68.90±1.37	<u>81.24</u> ±0.50	67.17±0.31	74.53±0.68	74.63±0.75	75.50±0.78	79.30±0.33	77.93±0.85	80.21±0.52	81.36 ±0.34
	Average	75.04	78.32	68.36	76.12	77.49	78.49	81.83	76.84	<u>82.17</u>	84.21
LOSO	BNCI2014001	73.64±1.14	72.22±1.03	73.21±1.79	72.56±0.96	71.76±0.75	73.40±1.22	73.07±2.01	69.62±1.32	<u>74.52</u> ±0.75	77.67 ±0.61
	BNCI2014004	67.78±0.92	62.19±0.79	62.56±0.56	67.09±0.69	65.17±0.66	65.28±1.09	64.22±1.05	63.15±1.42	67.69±0.43	69.85 ±0.47
	Zhou2016	83.22±1.83	82.10±0.67	83.84±1.18	82.07±0.91	82.09±1.31	83.88±1.03	82.43±1.48	84.06±1.58	86.21 ±0.99	<u>85.37</u> ±0.94
	Blankertz2007	71.10±0.83	70.64±0.58	72.19±0.89	<u>76.23</u> ±1.41	70.59±1.69	69.50±1.79	74.41±1.13	73.21±0.82	73.43±1.06	76.33 ±0.71
	BNCI2014002	72.86±0.38	70.57±1.35	<u>74.34</u> ±0.81	71.31±0.82	72.67±0.44	74.14±0.79	72.84±1.36	73.01±0.60	73.90±0.65	77.17 ±0.78
	Average	74.54	71.54	73.23	73.85	72.45	73.24	73.40	72.61	<u>75.15</u>	77.28

TABLE VI

AVERAGE CLASSIFICATION AUCs (%), F1s (%), AND BCAs (%) ON CHSZ AND NICU DATASETS UNDER THE LOSO SETTING. THE BEST AVERAGE PERFORMANCE IS MARKED IN BOLD, AND THE SECOND-BEST BY AN UNDERLINE.

Model	CHSZ			NICU		
	AUC	F1	BCA	AUC	F1	BCA
EEGNet	84.36	87.54	74.93	<u>71.87</u>	71.03	<u>64.79</u>
SCNN	49.17	70.18	50.15	68.86	76.54	63.52
DCNN	52.88	67.84	50.41	66.65	72.28	60.93
ADFCNet	86.49	<u>90.22</u>	<u>76.92</u>	70.48	69.45	62.60
EEG Conformer	<u>89.23</u>	88.01	74.33	71.46	<u>77.43</u>	64.04
SlimSeiz	86.94	87.56	76.30	71.78	70.01	64.25
EEGWaveNet	87.38	87.71	75.56	68.68	59.00	58.14
DBConformer	91.75	90.31	79.01	72.08	79.23	65.21

- *DBConformer extracted more structured and well-separated features.* With the integration of spatial encoding from the S-Conformer, DBConformer enhances the inter-class margins and promotes cluster compactness across all datasets, especially evident on BNCI2014001 and Blankertz2007.
- *The improvement is consistent across various MIs.* The benefit of dual-branch spatio-temporal modeling is observable regardless of categories (e.g., hand vs. hand/foot), demonstrating the generalization and robustness of the proposed design.

H. Interpretability of Channel Attention

To investigate the interpretability of the proposed channel attention module, we visualized the attention scores assigned to each EEG channel across 32 trials (a batch) from four MI datasets, illustrated in Fig. 6. We excluded BNCI2014004 from this analysis, as it only contains C3, Cz, and C4 channels and therefore lacks spatial coverage for attention comparison.

A consistent observation is that higher attention weights are repeatedly assigned to central motor-related channels, specifically C3, Cz, and C4, across all datasets. This aligns well with known neurophysiological principles of MI, where these central electrodes correspond to the sensorimotor cortex contralateral to movement imagination. Notably, even in different experimental setups, the model adaptively focuses on these physiologically relevant channels.

These results indicated that the proposed channel attention module can learn informative spatial priors in a data-driven manner, enhancing both performance and interpretability.

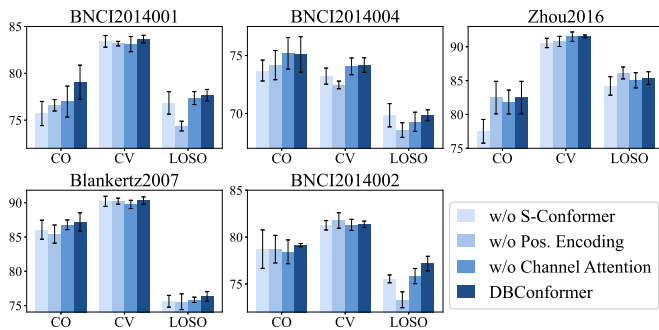


Fig. 4. Ablation studies on the parallel spatio-temporal design, positional encoding, and the channel attention module.

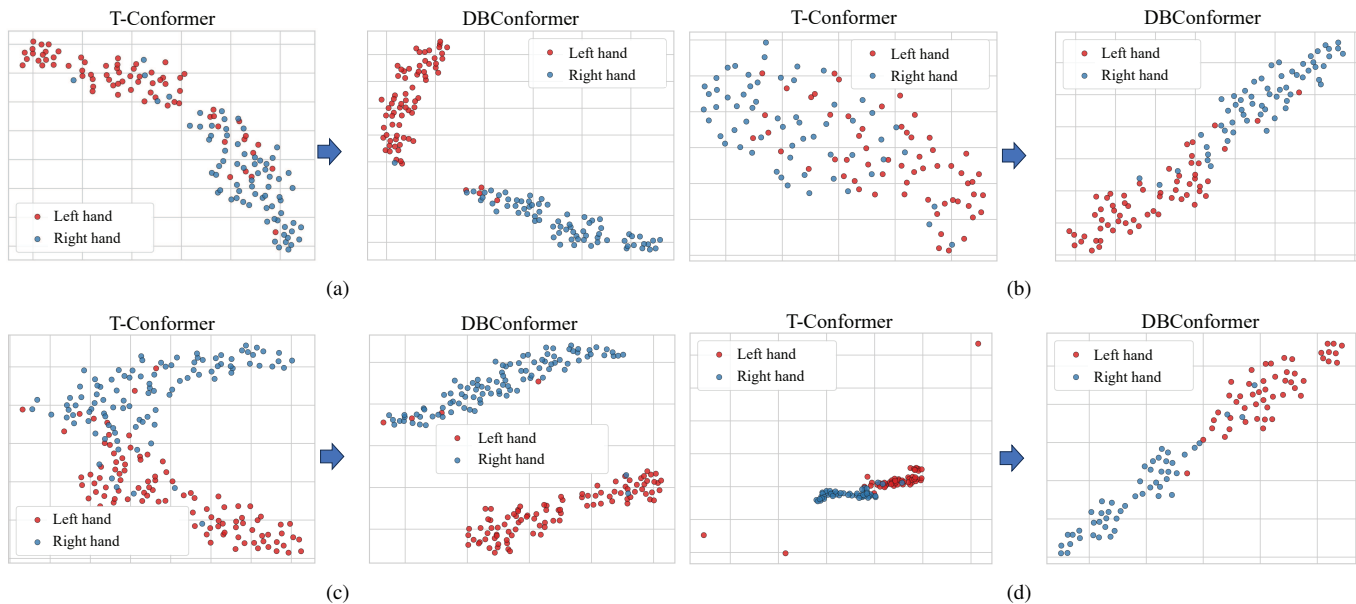


Fig. 5. t -SNE visualizations of features extracted from T-Conformer and DBConformer on (a) BNCI2014001, (b) BNCI2014004, (c) Blankertz2007, and (d) Zhou2016 datasets. Different categories are encoded by colors.

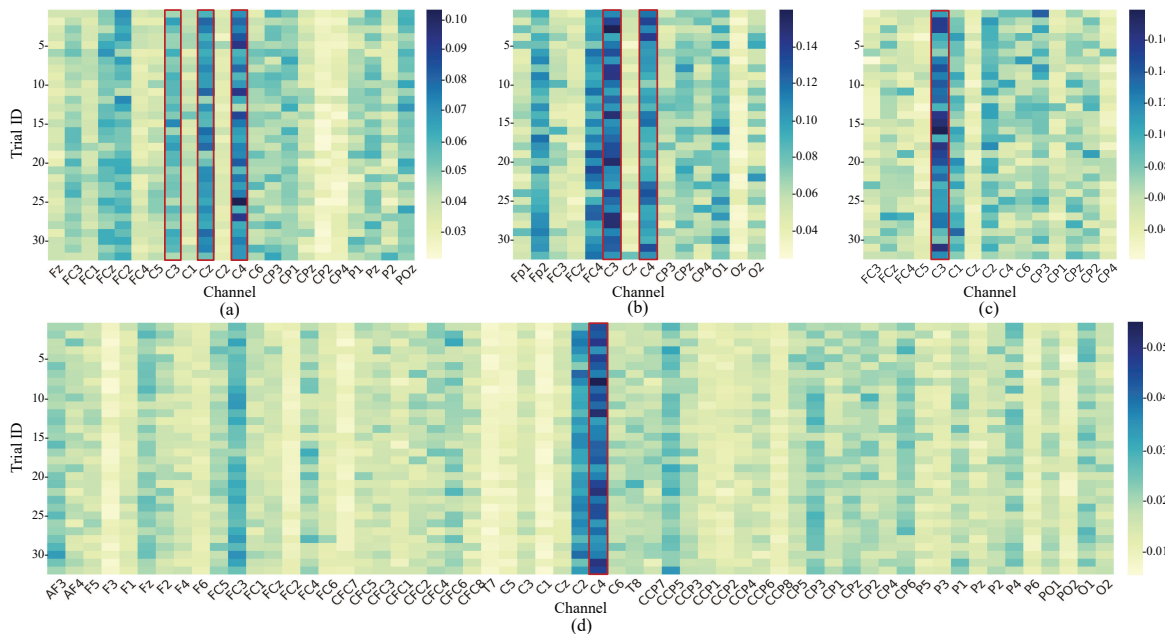


Fig. 6. Attention scores of each EEG channel calculated by the proposed channel attention module on (a) BNCI2014001, (b) Zhou2016, (c) BNCI2014002, and (d) Blankertz2007 datasets. The sum of scores from all channels of each sample is 1.

TABLE VII
COMPARISON OF MODEL COMPLEXITY AND PERFORMANCE METRICS ACROSS DBCONFORMER AND NINE BASELINE MODELS ON THE BNCI2014001 DATASET.

Metrics	CNN						CNN-Mamba	CNN-Transformer		
	EEGNet	SCNN	DCNN	FBCNet	ADFCNN	IFNet	SlimSeiz	CTNet	EEG Conformer	DBConformer (Ours)
# Model Parameters	1,406	46,084	320,479	7,042	4,322	7,748	27,650	27,284	789,668	92,066
Training Duration (s)	73.64	76.44	90.97	<u>70.45</u>	97.84	61.89	88.89	105.95	223.36	<u>203.79</u>
Accuracy (%)	73.64	72.22	73.21	72.56	71.76	<u>74.52</u>	69.62	73.40	73.07	77.67

I. Model Complexity and Performance Analysis

Table VII presents a comparative analysis of trainable parameter counts, training duration, and classification accuracy across DBConformer and nine baseline models. Observed that:

- Compared to lightweight CNN models, DBConformer introduces additional complexity due to the dual branches. Nonetheless, the trade-off in model size and training time is well-compensated by superior performance.
- DBConformer achieves the highest classification accuracy, surpassing all competing CNN and Conformer models. Despite incorporating a dual-branch Conformer design, it maintains a moderate number of parameters, with over $8\times$ fewer parameters than the high-capacity EEG Conformer.
- Overall, DBConformer demonstrates an effective balance between model capacity, computational efficiency, and accuracy, highlighting its suitability for EEG decoding.

V. CONCLUSION

This paper proposed DBConformer, a dual-branch convolutional Transformer network tailored for EEG decoding. It integrates a T-Conformer to model long-range temporal dependencies and an S-Conformer to enhance inter-channel interactions, capturing both temporal dynamics and spatial patterns in EEG data. A channel attention module further refines spatial characteristics by assigning data-driven importance to EEG channels. Comprehensive experiments on five MI datasets and two seizure detection datasets under three settings demonstrate that DBConformer consistently outperforms 10 competitive baseline models, with over $8\times$ fewer parameters than the high-capacity EEG Conformer baseline. Further, the visualization results confirm that the features extracted by DBConformer are physiologically interpretable and aligned with sensorimotor priors in MI.

In future work, DBConformer can be extended to support multi-view information fusion and plug-and-play real-time BCIs. Its superior performance and interpretability make it reliable for robust and explainable EEG decoding.

REFERENCES

- [1] J. V. Rosenfeld and Y. T. Wong, "Neurobionics and the brain-computer interface: current applications and future horizons," *Medical Journal of Australia*, vol. 206, no. 8, pp. 363–368, 2017.
- [2] D. Wu, Y. Xu, and B.-L. Lu, "Transfer learning for EEG-based brain-computer interfaces: A review of progress made since 2016," *IEEE Trans. on Cognitive and Developmental Systems*, vol. 14, no. 1, pp. 4–19, 2020.
- [3] G. Pfurtscheller and C. Neuper, "Motor imagery and direct brain-computer communication," *Proc. of the IEEE*, vol. 89, no. 7, pp. 1123–1134, 2001.
- [4] U. R. Acharya, S. V. Sree, G. Swapna, R. J. Martis, and J. S. Suri, "Automated EEG analysis of epilepsy: A review," *Knowledge-Based Systems*, vol. 45, pp. 147–165, 2013.
- [5] D. Wu, X. Jiang, and R. Peng, "Transfer learning for motor imagery based brain-computer interfaces: A tutorial," *Neural Networks*, vol. 153, pp. 235–253, 2022.
- [6] R. D. Thijs, R. Surges, T. J. O'Brien, and J. W. Sander, "Epilepsy in adults," *The Lancet*, vol. 393, no. 10172, pp. 689–701, 2019.
- [7] Z. Wang, W. Zhang, S. Li, X. Chen, and D. Wu, "Unsupervised domain adaptation for cross-patient seizure classification," *Journal of Neural Engineering*, vol. 20, no. 6, p. 066002, 2023.
- [8] V. J. Lawhern, N. R. Solon, Amelia J. and Waytowich, S. M. Gordon, C. P. Hung, and B. J. Lance, "EEGNet: A compact convolutional neural network for EEG-based brain-computer interfaces," *Journal of Neural Engineering*, vol. 15, no. 5, p. 056013, 2018.
- [9] R. T. Schirmeister, J. T. Springenberg, L. D. J. Fiederer, M. Glasstetter, K. Eggenberger, M. Tangermann, F. Hutter, W. Burgard, and T. Ball, "Deep learning with convolutional neural networks for EEG decoding and visualization," *Human Brain Mapping*, vol. 38, no. 11, pp. 5391–5420, 2017.
- [10] Y. Song, Q. Zheng, B. Liu, and X. Gao, "EEG Conformer: Convolutional transformer for EEG decoding and visualization," *IEEE Trans. on Neural Systems and Rehabilitation Engineering*, vol. 31, pp. 710–719, 2022.
- [11] W. Zhao, X. Jiang, B. Zhang, S. Xiao, and S. Weng, "CTNet: A convolutional transformer network for EEG-based motor imagery classification," *Scientific Reports*, vol. 14, no. 1, p. 20237, 2024.
- [12] Y. Ding, Y. Li, H. Sun, R. Liu, C. Tong, C. Liu, X. Zhou, and C. Guan, "EEG-Deformer: A dense convolutional transformer for brain-computer interfaces," *IEEE Journal of Biomedical and Health Informatics*, vol. 29, no. 3, 2024.
- [13] Z. Li, B. Chen, N. Zhu, W. Li, T. Liu, L. Guo, J. Han, T. Zhang, and Z. Yan, "Epileptic seizure detection in SEEG signals using a signal embedding temporal-spatial-spectral Transformer model," *IEEE Trans. on Instrumentation and Measurement*, vol. 74, pp. 1–11, 2025.
- [14] R. Mane, E. Chew, K. Chua, K. K. Ang, N. Robinson, A. P. Vinod, S.-W. Lee, and C. Guan, "FBCNet: A multi-view convolutional neural network for brain-computer interface," *arXiv preprint arXiv:2104.01233*, 2021.
- [15] J. Wang, L. Yao, and Y. Wang, "IFNet: An interactive frequency convolutional neural network for enhancing motor imagery decoding from EEG," *IEEE Trans. on Neural Systems and Rehabilitation Engineering*, vol. 31, pp. 1900–1911, 2023.
- [16] W. Tao, Z. Wang, C. M. Wong, Z. Jia, C. Li, X. Chen, C. P. Chen, and F. Wan, "ADFCNN: Attention-based dual-scale fusion convolutional neural network for motor imagery brain-computer interface," *IEEE Trans. on Neural Systems and Rehabilitation Engineering*, vol. 32, pp. 154–165, 2023.
- [17] Z. Wang, S. Li, X. Chen, W. Li, and D. Wu, "MVCNet: Multi-view contrastive network for motor imagery classification," *arXiv preprint arXiv:2502.17482*, 2025.
- [18] Z. Wang, S. Li, J. Luo, J. Liu, and D. Wu, "Channel reflection: Knowledge-driven data augmentation for EEG-based brain-computer interfaces," *Neural Networks*, vol. 176, p. 106351, 2024.
- [19] Q. Dong, Z. Wang, and M. Gao, "Noise-aware epileptic seizure prediction network via self-attention feature alignment," *IEEE Journal of Biomedical and Health Informatics*, pp. 1–13, 2025, early access.
- [20] Z. Wang, S. Li, X. Chen, and D. Wu, "Time-frequency transform based EEG data augmentation for brain-computer interfaces," *Knowledge-Based Systems*, vol. 311, p. 113074, 2025.
- [21] K. Liu, M. Yang, Z. Yu, G. Wang, and W. Wu, "FBMSNet: A filter-bank multi-scale convolutional neural network for EEG-based motor imagery decoding," *IEEE Trans. on Biomedical Engineering*, vol. 70, no. 2, pp. 436–445, 2022.
- [22] X. Jiang, L. Meng, X. Chen, Y. Xu, and D. Wu, "CSP-Net: Common spatial pattern empowered neural networks for EEG-based motor imagery classification," *Knowledge-Based Systems*, vol. 305, p. 112668, 2024.
- [23] B. Blankertz, R. Tomioka, S. Lemm, M. Kawanabe, and K.-r. Muller, "Optimizing spatial filters for robust EEG single-trial analysis," *IEEE Signal Processing Magazine*, vol. 25, no. 1, pp. 41–56, 2008.
- [24] K. Fu, J. Qu, Y. Chai, and Y. Dong, "Classification of seizure based on the time-frequency image of EEG signals using HHT and SVM," *Biomedical Signal Processing and Control*, vol. 13, pp. 15–22, 2014.
- [25] M. Mursalin, Y. Zhang, Y. Chen, and N. V. Chawla, "Automated epileptic seizure detection using improved correlation-based feature selection with random forest classifier," *Neurocomputing*, vol. 241, pp. 204–214, 2017.
- [26] P. Thuwajit, P. Rangpong, P. Sawangjai, P. Autthasan, R. Chaisaen, N. Banluesombatkul, P. Boonchit, N. Tatsaringkankasakul, T. Sudhawiyangkul, and T. Wilaiprasitporn, "EEGWaveNet: Multiscale CNN-based spatiotemporal feature extraction for EEG seizure detection," *IEEE Trans. on Industrial Informatics*, vol. 18, no. 8, pp. 5547–5557, 2022.
- [27] Y. Gui, M. Chen, Y. Su, G. Luo, and Y. Yang, "EEGMamba: Bidirectional state space model with mixture of experts for EEG multi-task classification," *arXiv preprint arXiv:2407.20254*, 2024.
- [28] M. Guo, X. Han, H. Liu, J. Zhu, J. Zhang, Y. Bai, and G. Ni, "MI-Mamba: A hybrid motor imagery electroencephalograph classification

- model with Mamba’s global scanning,” *Annals of the New York Academy of Sciences*, vol. 1544, no. 1, pp. 242–253, 2025.
- [29] Q. Deng, Q. Wang, W. Liu, and Y. Xue, “EEG VMamba: Vision mamba for seizure prediction based on EEG,” in *Procs. of the Int’l Conf. on Video, Signal and Image Processing*, Ningbo, China, Nov. 2024, pp. 119–124.
- [30] G. Lu, J. Peng, B. Huang, C. Gao, T. Stefanov, Y. Hao, and Q. Chen, “SlimSeiz: Efficient channel-adaptive seizure prediction using a Mamba-enhanced network,” *arXiv preprint arXiv:2410.09998*, 2024.
- [31] X. Zhou, Y. Han, Z. Chen, C. Liu, Y. Ding, Z. Jia, and Y. Liu, “BiT-MamSleep: Bidirectional temporal Mamba for EEG sleep staging,” *arXiv preprint arXiv:2411.01589*, 2024.
- [32] A. Gu and T. Dao, “Mamba: Linear-time sequence modeling with selective state spaces,” *arXiv preprint arXiv:2312.00752*, 2023.
- [33] J. Xie, J. Zhang, J. Sun, Z. Ma, L. Qin, G. Li, H. Zhou, and Y. Zhan, “A transformer-based approach combining deep learning network and spatial-temporal information for raw EEG classification,” *IEEE Trans. on Neural Systems and Rehabilitation Engineering*, vol. 30, pp. 2126–2136, 2022.
- [34] C. Ju and C. Guan, “Graph neural networks on spd manifolds for motor imagery classification: A perspective from the time–frequency analysis,” *IEEE Trans. on Neural Networks and Learning Systems*, vol. 35, no. 12, pp. 17701–17715, 2023.
- [35] S. Cai, H. Li, Q. Wu, J. Liu, and Y. Zhang, “Motor imagery decoding in the presence of distraction using graph sequence neural networks,” *IEEE Trans. on Neural Systems and Rehabilitation Engineering*, vol. 30, pp. 1716–1726, 2022.
- [36] D. Zhang, K. Chen, D. Jian, and L. Yao, “Motor imagery classification via temporal attention cues of graph embedded EEG signals,” *IEEE Journal of Biomedical and Health Informatics*, vol. 24, no. 9, pp. 2570–2579, 2020.
- [37] H. He and D. Wu, “Transfer learning for brain-computer interfaces: A Euclidean space data alignment approach,” *IEEE Trans. on Biomedical Engineering*, vol. 67, no. 2, pp. 399–410, 2020.
- [38] A. Vaswani, N. Shazeer, N. Parmar, J. Uszkoreit, L. Jones, A. N. Gomez, L. Kaiser, and I. Polosukhin, “Attention is all you need,” in *Proc. Advances in Neural Information Processing Systems*, Long Beach, CA, USA, Dec. 2017.
- [39] S. Chevallier, I. Carrara, B. Aristimunha, P. Guetschel, S. Sedlar, B. Lopes, S. Velut, S. Khazem, and T. Moreau, “The largest EEG-based BCI reproducibility study for open science: the MOABB benchmark,” *arXiv preprint arXiv:2404.15319*, 2024.
- [40] M. Tangermann, K.-R. Müller, A. Aertsen, N. Birbaumer, C. Braun, C. Brunner, R. Leeb, C. Mehring, K. J. Miller, G. R. Müller-Putz *et al.*, “Review of the BCI competition IV,” *Frontiers in Neuroscience*, vol. 6, p. 55, 2012.
- [41] R. Leeb, F. Lee, C. Keinrath, R. Scherer, H. Bischof, and G. Pfurtscheller, “Brain–computer communication: motivation, aim, and impact of exploring a virtual apartment,” *IEEE Trans. on Neural Systems and Rehabilitation Engineering*, vol. 15, no. 4, pp. 473–482, 2007.
- [42] B. Zhou, X. Wu, Z. Lv, L. Zhang, and X. Guo, “A fully automated trial selection method for optimization of motor imagery based brain-computer interface,” *PloS One*, vol. 11, no. 9, p. e0162657, 2016.
- [43] B. Blankertz, G. Dornhege, M. Krauledat, K.-R. Müller, and G. Curio, “The non-invasive Berlin brain–computer interface: fast acquisition of effective performance in untrained subjects,” *NeuroImage*, vol. 37, no. 2, pp. 539–550, 2007.
- [44] D. Steyrl, R. Scherer, J. Faller, and G. R. Müller-Putz, “Random forests in non-invasive sensorimotor rhythm brain-computer interfaces: a practical and convenient non-linear classifier,” *Biomedical Engineering/Biomedizinische Technik*, vol. 61, no. 1, pp. 77–86, 2016.
- [45] N. J. Stevenson, K. Tapani, L. Lauronen, and S. Vanhatalo, “A dataset of neonatal EEG recordings with seizure annotations,” *Scientific Data*, vol. 6, no. 1, pp. 1–8, 2019.
- [46] S. Li, Z. Wang, H. Luo, L. Ding, and D. Wu, “T-TIME: Test-time information maximization ensemble for plug-and-play BCIs,” *IEEE Trans. on Biomedical Engineering*, vol. 71, no. 2, pp. 423–432, 2024.
- [47] L. Van der Maaten and G. Hinton, “Visualizing data using t-SNE,” *Journal of Machine Learning Research*, vol. 9, no. 11, pp. 2579–2605, 2008.